THE ELECTRONIC RELAXATION OF THE S_1 SINGLET STATE OF HEXAFLUOROBIACETYL IN THE VAPOUR PHASE

A. PETIT and R. BOTTER

Département de Physicochimie, Centre d'Etudes Nucléaires de Saclay, B.P. 2, 91190 Gif-sur-Yvette (France)

(Received January 14, 1981; in revised form April 6, 1981)

Summary

The time-resolved fluorescence of hexafluorobiacetyl (CF_3—CO—CO—CF_3) was studied at pressures down to 0.05 Torr over the excitation energy range 22000 - 30000 cm^{-1}. The zero-pressure fluorescence lifetime and the pressure effect as functions of energy were measured. The energy dependence of the fluorescence radiative rate k_s^{rad} was determined from the fluorescence quantum yield measurements at low and high pressures. By means of a Rice–Ramsperger–Kassel–Marcus calculation the dissociation process was shown to be important compared with intersystem crossing and internal conversion only for energies greater than 28000 cm^{-1}.

These results are in good agreement with those published by Van der Werf and Kommandeur on biacetyl.

1. Introduction

Although the photophysics and photochemistry of simple dicarbonyls (see, for example, ref. 1) have been studied extensively, they are not well understood (especially the behaviour of non-radiative processes). For example for biacetyl a collision-independent singlet–triplet process with a rate corresponding to $k_{ST} = 7.6 \times 10^7$ s^{-1} has been reported [2 - 4]. This high rate could not be explained in terms of the density of triplet vibronic states, as required by the theory of radiationless transitions [5].

Recently, the important work by Van der Werf and Kommandeur [6] has helped in the solution of this problem; these researchers have analysed the photophysical behaviour of methyl glyoxal and biacetyl (biexponential behaviour) according to the theory for "intermediate case" molecules of Lamani *et al.* [7].

In another paper Van der Werf *et al.* [8] have compared the photophysical behaviours of the dicarbonyls glyoxal, methyl glyoxal and biacetyl and have shown that in all three cases the total decay was dominated by non-radiative processes. In order to complete this study on simple dicarbonyls, in this work we examine the photophysical behaviour of hexafluorobiacetyl

(HFB), CF_3—CO—CO—CF_3. This molecule absorbs in the same spectral range as does biacetyl (330 - 460 nm) and fluoresces between 450 and 600 nm. The presence of fluorine atoms must considerably increase the density of triplet states (for instance at the exciting wavelength λ_{ex} = 385 nm, the density of states $\rho_T \approx 3 \times 10^3$ states per wavenumber for biacetyl and $\rho_T \approx 3 \times 10^6$ states per wavenumber for HFB).

It is interesting to study the influence of fluorine atoms on the fluorescence decay. We should notice an important decrease in the total non-radiative rate constant k_{NR}, as occurs for simple analogous ketones under identical excitation conditions (acetone, k_{NR} = 3.1 $\times 10^8$ s^{-1}; hexafluoro-acetone, k_{NR} = 1.2 $\times 10^7$ s^{-1}; cyclobutanone, k_{NR} = 2 $\times 10^8$ s^{-1}; perfluoro-cyclobutanone, k_{NR} = 9 $\times 10^6$ s^{-1}).

In this paper, we report only the fast fluorescence behaviour. After a discussion of the experiments and their interpretation, we compare our results with those obtained with HFB by McIntosh and coworkers [9] and Reid and coworkers [10] who studied respectively the emission quantum yields and the dissociation quantum yields. We then compare our data with the results of Van der Werf and Kommandeur on biacetyl [6].

2. Experimental details

2.1. Sample handling

The gases were handled in a standard glass vacuum line with a background pressure of less than 10^{-5} Torr. The Pyrex fluorescence cell was spherical, 15 cm in diameter.

2,3-Dichloro-1,1,1,4,4,4-hexafluoro-2-butene was first prepared with the method of Henne and Trot [11] and then distilled with a 10-plate column. No impurity was detected by IR and fluorine nuclear magnetic resonance (NMR) spectroscopy. HFB was prepared by chromic acid oxidation of the 2,3-dichloro-1,1,1,4,4,4-hexafluoro-2-butene [12]. The crude condensate was purified by trap-to-trap distillation in vacuo from −78 °C (methanol–carbon dioxide) to −96 °C (toluene–liquid nitrogen). This procedure was repeated several times.

No impurity was detected in the product by fluorine and proton NMR spectroscopy. The principal impurities detected by mass spectroscopy were the olefin and trifluoroacetyl chloride. After several trap-to-trap distillations the amount of these impurities was less than 2%.

The HFB was stored in blackened bulbs with greaseless stopcocks at −78 °C. Argon (N 55) was supplied by Air Liquide. Pressures in the range 10 - 10^{-2} Torr were measured with a capacitance manometer (Barocel–Datametrics, 10 Torr head).

2.2. Optical system

The excitation source used was a pulsed dye laser (Jobin–Yvon spectrolas 3 A) pumped by a nitrogen laser as described elsewhere [13].

The following dye solutions supplied by Jobin–Yvon were used: Coumarine 120 in ethanol (455 - 425 nm); 2-(4-biphenyl)-6-phenylbenzoxazole (PBBO) in toluene–ethanol (425 - 400 nm); 4,4'''-bis(2-butyl)-octyloxy)-p-quaterphenyl (Bi Buq) in toluene (399 - 385 nm); 2-(4-biphenyl)-5-(p-tert-butylphenyl)-1,3,4-oxadiazole (Butyl PBD) in toluene–ethanol (385 - 366 nm).

The spectral width was typically 0.3 nm and the pulse energy (70 - 250 μJ) was measured with a joule meter (Laser Precision Corp., model RJ 7100) equipped with an RJP 134 pyroelectric head. The pulse duration was 2.5 ns (full width at half-maximum). The fluorescence light, perpendicular to the excitation beam, was collected with a lens as indicated in Fig. 1.

Before passing into a Bausch and Lomb monochromator (300 Å spectral width), the beam was attenuated with neutral optical density filters (MTO Densivex, linear over the range 200 - 800 nm) in order to normalize the number of photons collected at each wavelength on the photocathode of the photomultiplier (PM). The fluorescence light was detected with a PM (XP 2020 from RTC) with an S 20 cathode and a nominal rise time of 2.5 ns.
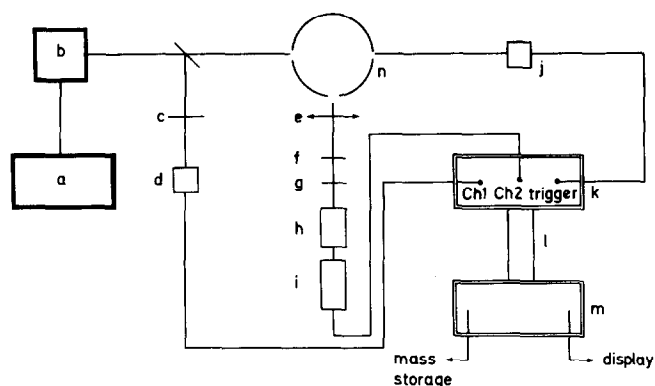

Fig. 1. A schematic diagram of the experimental system: a, nitrogen laser; b, dye laser; c, g, neutral density filters; j, d, photodiode; e, lens; f, filter; h, monochromator; i, photomultiplier; k, programmable digitizer; m, minicomputer; l, interface system; n, fluorescence cell.

2.3. Electronic system

The current pulse from the PM tube passed through a load resistor (50 Ω) and the output signal was digitized with a Tektronix R 7912 transient digitizer with 512 vertical and 512 horizontal channels.

The time base was triggered by a vacuum photodiode (j) pulse as indicated in Fig. 1. This signal was developed by the dye laser pulse after its passage through the fluorescence cell. The time base was accurate to better than 4%.

Signal averaging at 1 Hz was accomplished with a PDP 11 computer and Tektronix WDI software. The overall system response time determined by the decay time of scattered light was 4 ns.

2.4. Experimental procedure

A small part of the excitation signal D coming from the photodiode d was averaged over 300 shots. This signal was used as a reference for normalization of the fluorescence intensity. After pumping the fluorescence cell, the scattered light signal B was averaged over the same number of shots; then the cell was filled with gas and the observed signal A was averaged under identical conditions.

Although the peak intensity of the scattered light was as much as three times greater than the true fluorescence signal intensity for the lowest pressure studied, the scattered light decayed much more rapidly than the fluorescence signal (except for λ_{ex} = 337.1 nm). The final curve C was obtained by digitally subtracting the scattered light B from signal A (fluorescence plus scattered light).

Care was always taken to keep the number of photons arriving on the PM tube almost constant in order to maintain the same vertical signal amplitude (180 - 300 mV). This procedure avoids problems which arise from the geometric defects of the R 7912 tube and from the calibration of the vertical amplifier; such conditions enable us to work with the maximum accuracy of the system, $\pm 3\%$. The analysis of the decay times was performed with a non-linear least-squares program which we have written. A statistical analysis of the results was also included in this program.

Quantum yields were calculated in the following manner. The mean integrated fluorescence intensity is given by the area under the curve C, so the time-averaged integrated emission intensities for the collision and relaxed experiments are respectively

$$I_{tot}^{cf} = \int_{0}^{5\tau_{\nu}^{cf}} I^{cf}(0) \exp\left(-\frac{t}{\tau_{\nu}^{cf}}\right) dt \tag{1}$$

and

$$I_{tot}^{r} = \int_{0}^{5\tau^{r}} I^{r}(0) \exp\left(-\frac{t}{\tau^{r}}\right) dt \tag{2}$$

where $I^{cf}(0)$ and $I^{r}(0)$ are the intensities at time zero and τ is the fluorescence lifetime; cf denotes collision free, ν denotes the initial vibronic level excited and r denotes the relaxed state. If the laser intensity were constant between the two measurements, the relative quantum yield would be

$$\frac{\phi_{\nu}^{cf}}{\phi^{r}} = \frac{I_{tot}^{cf}}{I_{tot}^{r}}$$

However, the laser intensity was not constant over the two sets of experiments and so we define the mean integrated laser intensity (area under the excitation decay curve D) in an analogous manner to the fluorescence intensities defined above:

$$L_{tot}{}^{cf} = \int\limits_{0}^{5\tau_L} L^{cf}(0) \exp\left(-\frac{t}{\tau_L}\right) dt \qquad (3)$$

and

$$L_{tot}{}^{r} = \int\limits_{0}^{5\tau_L} L^{r}(0) \exp\left(-\frac{t}{\tau_L}\right) dt \qquad (4)$$

where $L(0)$ is the laser intensity at time $t = 0$ and τ_L is the mean lifetime of the decay curve D. This signal originates from the convolution product of the true laser pulse with the apparatus function of the observation system.

This method is appropriate in the sense that we measure a ratio and that no corrections for wavelength sensitivity of the PM tube are necessary. Moreover, these quantum yield measurements are time resolved; this procedure enables us to measure the true relative quantum yield of the observed emission. If no corrections for absorption are needed, the ratio of the two relative quantum yields is simply given by [14]

$$\frac{\phi^{cf}}{\phi^r} = \frac{I_{tot}{}^{cf}}{I_{tot}{}^{r}} \frac{L_{tot}{}^{r}}{L_{tot}{}^{cf}} \qquad (5)$$

In our experiments this ratio was measured as follows. The ratio integral (C): integral (D) was first determined at a low pressure; then argon at 760 Torr was added to the fluorescence cell and the ratio was again determined after waiting 20 min to allow complete homogenization.

2.5. Calibration of the decay time measurements

It seemed necessary to us to check the ability of the system to measure short fluorescence decay times: the fluorescence lifetimes of three different compounds were measured and compared with known values given in the literature (Table 1).

TABLE 1

Fluorescence decay time values of three known compounds

Compound	This work[a] (ns)	Literature value (ns)
Hexafluoroacetone (gas)	67 ± 2 (at 0.2 Torr)	69 (at 0.2 Torr; λ_{ex} = 337.1 nm) [15]
	83 ± 3 (at 20 Torr)	70 (at 0.2 Torr; λ_{ex} = 337.1 nm) [16]
		84 (at 0.2 Torr; λ_{ex} = 357.7 nm) [17]
Quinine bisulphate (liquid)[b]	20 ± 0.6	19.4 [18]
		20.1 [19]
1,6-Diphenyl-1,3,5-hexatriene (liquid)[c]	10.5 ± 0.3	12.4 (λ_{ex} = 365 nm) [20]

[a] All measurements were performed with λ_{ex} = 337.1 nm.
[b] 1 N in sulphuric acid.
[c] 0.1 g l^{-1} in cyclohexane.

3. Results

3.1. Fluorescence decay time measurements of hexafluorobiacetyl

In the time range that is important for fluorescence, the intensity of phosphorescence is negligible. The pressure dependence of the fluorescence decay for different excitation wavelengths is shown in Fig. 2. These curves have the same shape as those predicted by McIntosh and coworkers [9] for the fluorescence yield.

At 100 Torr the vibrational relaxation is almost complete and independent of the excitation wavelength. The lifetime does not increase further even if we add argon at 1 atm (points indicated at 1000 Torr in Fig. 2: only a few points are shown). At this pressure and at greater pressures the decay is purely exponential.

No other variation in the lifetime is seen at pressures lower than 1 Torr, so we can consider these lifetimes as zero-pressure rates; moreover, if we suppose a gas kinetic collision diameter of 7 Å for hard sphere collisions, the collision-free lifetime always exceeds the fluorescence lifetime by a factor of 20 or more. Under such collision-free conditions the decay is again exponential.

Between 1 and 100 Torr non-exponential decays are observed owing to the vibrational relaxation. However, these decays are almost exponential and are analysed as such over two decades. It can be noticed that, for an excitation
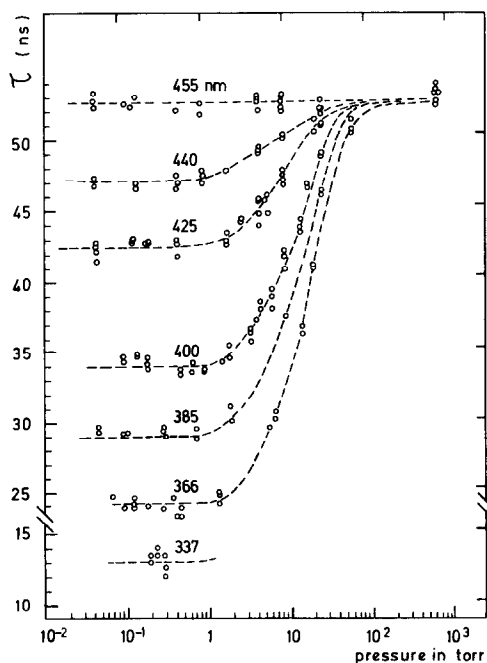

Fig. 2. The dependence of the fluorescence lifetime on hexafluorobiacetyl pressure for different excitation wavelengths.

wavelength of 455 nm, no change in fluorescence lifetime τ_F (within experimental errors) is observed with pressure: this lifetime corresponds to the decay of the vibrationally relaxed S_1 state.

The location of the 0–0 band can be estimated to be 22000 cm^{-1} in agreement with the value of McIntosh and coworkers [9]. Moreover, the value estimated for HFB should be similar to the value found for biacetyl (22200 cm^{-1}) since only a slight red shift is observed in the absorption and fluorescence spectra of HFB compared with those of biacetyl.

The energy dependence of the zero-pressure fluorescence rate is given in Fig. 3 and Table 2. (The lifetime measurement with the excitation wavelength of 337.1 nm was made with the nitrogen laser source ($\Delta\lambda \approx 0.2$ nm).)
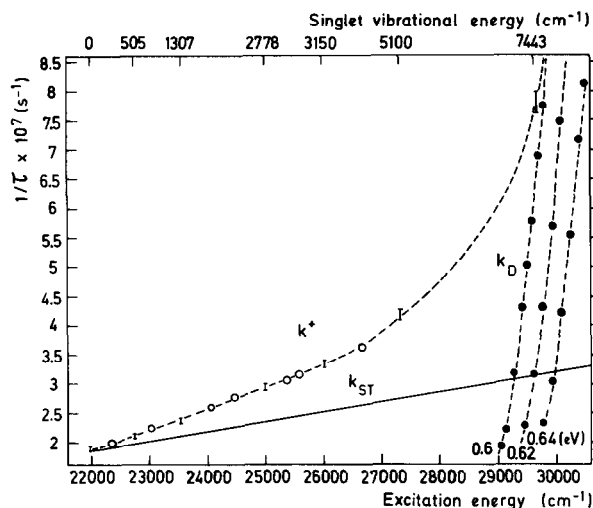

Fig. 3. The observed fluorescence rate as a function of excitation energy (in wavenumbers): $-\bigcirc-$, k^+; ——, k_{ST}; $-\bullet-$, k_D (the meanings of k^+, k_{ST} and k_D are indicated in the text).

3.2. Calculation of the dissociation rate constant

The specific rate constant for dissociation of the singlet excited state S_1 with total internal energy ϵ^* is given, according to the Marcus theory [21], by

$$k_D(\epsilon^*) = \frac{1}{h} \frac{Z^+}{Z^*} \frac{S^+(\epsilon^+)}{N^*(\epsilon^*)} \tag{6}$$

where

$$\epsilon^* = \epsilon_x + \epsilon_{Boltzmann}$$

$$\epsilon^+ = \epsilon_x - \epsilon_{min} + \epsilon_{Boltzmann}$$

ϵ_x is the difference in energy between the exciting wavelength and the 0–0 energy ϵ_0. Z^+/Z^* is the ratio of the partition functions for adiabatic degrees of freedom of the activated complex and of the excited molecule. ϵ_{min} is the critical dissociation energy. $S^+(\epsilon^+)$ is the sum of all energy states for the

TABLE 2

The energy dependence of the zero-pressure rate of fluorescence

Excitation wavelength (nm)	Wavenumber (cm^{-1})	$k^{+a} \times 10^7$ (s^{-1})
455.0	21978	1.90
447.5	22346	1.98
440.0	22727	2.13
432.5	23121	2.24
425.0	23529	2.36
415.0	24096	2.60
408.5	24480	2.77
400.0	25000	2.94
392.5	25478	3.06
391.0	25575	3.16
385.0	25974	3.45
375.0	26666	3.62
366.0	27322	4.13
337.1	29665	7.8

[a]Zero-pressure rate of fluorescence:

$$k^+(\epsilon) = k_s^{\text{rad}}(\epsilon) + k_{ST}(\epsilon) + k_{IC}(\epsilon) + k_D(\epsilon)$$

or

$$k^+(\epsilon) = k_s^{\text{rad}}(\epsilon) + k_{NR}$$

with

$$k_{NR}(\epsilon) = k_{ST}(\epsilon) + k_{IC}(\epsilon) + k_D(\epsilon)$$

active vibration–rotation degrees of freedom of the activated complex up to its energy ϵ^+ whilst $N^*(\epsilon^*)$ is the corresponding density of states for the excited molecule. $\epsilon_{\text{Boltzmann}}$ is the thermal energy of the ground state.

The functions S^+ and N^* have been calculated using Haaroff's [22] formula. Although a complete vibrational analysis for HFB has not been made, most of the normal mode frequencies can be reasonably well estimated by comparison with related species such as biacetyl, acetone and hexafluoroacetone (see Appendix A). For the excited state, those frequencies which are closely associated with the region of electronic excitation have been reduced by 20% (C=O stretching modes) by comparison with the work of Sidman and McClure [23] on biacetyl. The non-torsional motions of the CF$_3$ groups have been assigned frequencies that are 10% less than the corresponding ground state values. Vibrational frequencies for the activated complex have been taken to be the same as those for the excited molecule, omitting the symmetric central C—C stretching mode which becomes the reaction coordinate as the molecule dissociates into two CF$_3$CO radicals.

Overall rotations have been assumed to be adiabatic with Z^+/Z^* equal to unity. The calculations have been performed for different values of the activation energy ϵ_{min} as indicated in Fig. 3. The most realistic value of ϵ_{min} must be governed by two conditions.

(1) The dissociation process at $\lambda_{\text{ex}} = 337.1$ nm should be very important relative to other non-radiative processes. Reid and coworkers [10] gave a

value $k_D = 0.5 \times 10^8$ s^{-1} for the singlet dissociation at $\lambda_{ex} = 334$ nm (this value has been measured by three different methods) and we have found that $k^+ = 0.78 \times 10^8$ s^{-1} (total non-radiative rate constant) at $\lambda_{ex} = 337.1$ nm. (The magnitude of k_s^{rad} is of the order of 10^5 s^{-1} for dicarbonyl compounds. This constant can be neglected compared with k_{NR} (10^7 - 10^8 s^{-1}), so the constant k^+ will be compounded with k_{NR}.) The dissociation curve should in fact be asymptotic to the curve $k^+ = f(\epsilon_{exc})$. This condition gives an upper limit for ϵ_{min} values ($\epsilon_{min} < 0.64$ eV) (Fig. 3).

(2) The value of the dissociation rate constant must be less than or equal to the total non-radiative rate constant k_{NR}^{tot}; this gives a lower limit for ϵ_{min} values. We can see in Fig. 3 that ϵ_{min} must be larger than 0.6 eV.

If we take these two conditions into account the best results are obtained for $\epsilon_{min} = 0.62$ eV.

A decrease of 10% in all vibrational frequencies changes the dissociation rate constant by only a factor of 2. The calculations are very approximate and are subject to the uncertainties present in applying the Rice–Ramsperger–Kassel–Marcus theory to photodissociation (all these uncertainties have already been discussed elsewhere [24]) but they indicate that the dissociation process in the singlet state is only competitive with other non-radiative processes for energies greater than 28000 cm^{-1}. The trend in the total non-radiative constant k_{NR} ($1/\tau_F$) with excitation energies less than 28000 cm^{-1} can only be explained by the energy dependence of the two competitive non-radiative processes (intersystem crossing and internal conversion).

3.3. Fluorescence quantum yield measurement

(a) The Lambert–Beer law agreement was checked for three different excitation wavelengths (450, 415 and 385 nm) and five different optical densities.

(b) As only a small part (30 nm) of the total fluorescence emission was observed through the monochromator we have checked, for two excitation wavelengths (385 and 400 nm), that the fluorescence spectra in collision-free and relaxed conditions were identical in shape within experimental error (no displacement was observed).

· These spectra are presented in Fig. 4 for $\lambda_{ex} = 385$ nm where the fluorescence lifetimes are different by a factor of almost 2.

(c) With a multireflection cell, the effect of argon at 1 atm on the HFB absorption coefficient was measured for different excitation wavelengths. In all cases, the effect due to the addition of argon was less than 10% so that the fluorescence yields presented in Table 3 are not corrected.

Under such conditions, it is possible to apply eqn. (5) to the relative fluorescence yield measurements. Using the same notation as Van der Werf and Kommandeur [6], we can write

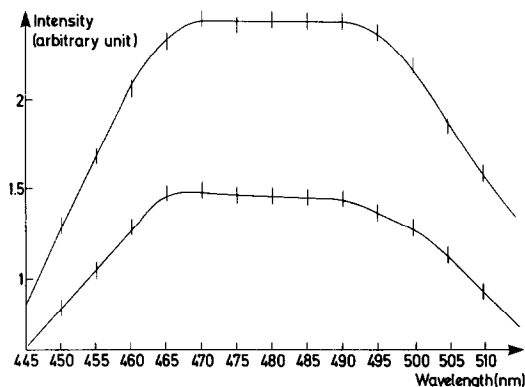$$\frac{\phi^{cf}(\epsilon,0)}{\phi^{cf}(\epsilon_0,0)} = \frac{k_s^{rad}(\epsilon,0)}{k_s^{rad}(\epsilon_0,0)} \frac{k^+(\epsilon_0,0)}{k^+(\epsilon,0)} \tag{7}$$

Fig. 4. Fluorescence spectra of HFB (λ_{ex} = 385 nm; $\Delta\lambda_{obs}$ = 5 nm): lower curve, HFB at 0.3 Torr; upper curve, HFB at 0.3 Torr plus argon at 760 Torr.

TABLE 3

The change in the zero-pressure singlet radiative rate constant with energy

Excitation energy ϵ_0 (cm^{-1})	$\dfrac{\phi^{cf}(\epsilon,0)}{\phi^r(\epsilon,\infty)}$	$\dfrac{\phi^{cf}(\epsilon,0)}{\phi^{cf}(\epsilon_0,0)}$	$\dfrac{k^+(\epsilon_0,0)}{k^+(\epsilon,0)}$	$\dfrac{k_S^{rad}(\epsilon,0)}{k_S^{rad}(\epsilon,0)}$
21978	0.85	1	1	1
22727	0.87	1.02	0.89	1.1
23929	0.75	0.88	0.8	1.1
25000	0.72	0.85	0.65	1.3
25976	0.61	0.72	0.55	1.3
27322	0.55	0.65	0.46	1.4
Typical errors	±10%	±10%	±10%	±20%

The excitation energy and pressure dependences of the relative fluorescence yields, the radiative rate and the fast fluorescence rate are expressed respectively as $\phi(\epsilon, p)$, $k_s^{rad}(\epsilon, p)$ and $k^+(\epsilon, p)$. ϵ_0 is the excitation energy of the relaxed singlet state S_1.

Since we know the ratio of the zero-pressure fluorescence yields for different excitation energies and the dependence of k^+ on ϵ (Table 2), we can deduce the change in k_s^{rad} as a function of energy (Table 3). Fleming et al. [25] have shown that, within the harmonic oscillator approximation for both symmetry-allowed and symmetry-forbidden transitions, k_s^{rad} should vary linearly with the excess vibrational energy in the excited state. k_s^{rad} may increase or decrease with excess energy depending on vibrational frequency changes and the nature of the modes excited.

If we suppose that there is a linear relation between k_s^{rad} and ϵ, the values in Table 3 show that k_s^{rad} increases by about 40% over the spectral range 21978 - 27322 cm^{-1}. This is in good agreement with the result of

Van der Werf and Kommandeur [6] who found an increase of 30% for biacetyl over the same spectral range. In agreement with the findings of Van der Werf and Kommandeur [6], the fluorescence was almost independent of the exciting wavelength and argon pressure (Fig. 4).

4. Analysis of the data

4.1. Radiative rates

McIntosh and coworkers [9] have shown that the thermalized (high pressure) triplet yield (λ_{ex} = 436 nm) $k_{ST}(436)/k^+(436)$ was equal to that of hexafluoroacetone, *i.e.* almost unity. As for biacetyl it can be concluded that at $\lambda_{ex} > 436$ nm intersystem crossing is the most probable process and all other processes are negligible compared with k_{ST}, so from

$$\phi^{cf}(\lambda_{ex} = 436 \text{ nm}; p = 0) = 4.8 \times 10^{-3} \tag{8}$$

and our value for $k^+(\epsilon_0, p = 0)$ of 1.9×10^7 s$^{-1} \approx k_{ST}(\epsilon_0, p = 0)$, we can calculate the zero-pressure singlet radiative rate. For $\epsilon_0 = 21978$ cm^{-1}, we have $k_s^{rad}(\epsilon_0, p = 0) = 9.3 \times 10^4$ s^{-1}. This value compares reasonably well with that (1.5×10^5 s^{-1}) of McIntosh and coworkers [9] calculated from the integrated absorption coefficient (these researchers used this calculated value to evaluate the lifetime of the thermalized S_1 singlet state (32 ns)).

Knowing the value of $k_s^{rad}(\epsilon_0, 0)$ we can deduce (from Section 3.3) the complete variation in the radiative rate constant k^{rad} with energy.

4.2. Energy dependence on k_{ST}

At low energies, k_{ST} is almost equal to k^+ (Section 4.1), *i.e.* $k_{ST} = 1.9 \times 10^7$ s^{-1}. For higher energies we use the relation given by Van der Werf and Kommandeur [6] (Section 5.2):

$$\frac{k_{ST}\phi/k^+}{k_s^{rad}/k^+} = \frac{\phi_{ph}^{th}(p = \infty)}{\phi^{cf}(p = 0)} \tag{9}$$

where $\phi = k_T^{rad}/k_T^{th}$ is the phosphorescence yield relative to the number of thermalized triplets. (k_T^{rad} is the phosphorescence radiative rate and k_T^{th} is the decay rate of the thermalized triplet T_1 state.) $\phi_{ph}^{th}(p = \infty)$ is the yield of the thermalized phosphorescence per excited molecule. Since McIntosh and coworkers [9] have shown that $\phi_{ph}^{th}(p = \infty)/\phi^{cf}(p = 0)$ and ϕ ($\phi = 0.078$) were independent of the excitation, we can conclude as for biacetyl that k_{ST} has the same dependence on energy as does k_s^{rad} (Table 4 and Fig. 3). Contrary to the studies of McIntosh and Reid, which neglected internal conversion ($S_1 \rightarrow S_0$) processes, the present results clearly show the importance of internal conversion in HFB since the dissociation process (Section 3.2) only competes in the S_1 state, with intersystem crossing and internal conversion at energies greater than 27322 cm^{-1} (366 nm). Knowing the energy dependence of k_{ST}, we deduce that $k_{IC} \approx k^+ - k_{ST}$: this procedure gives an approximate value of k_{IC} and its energy dependence (Table 4).

TABLE 4

Values of the non-radiative rate constants

λ_{ex} (nm)	Non-radiative rate constants ($\times 10^{-7}$ s^{-1})		
	This work	[9]	[10]
455	$k_{ST} = 1.9$		
440	$k^+ = 2.12$ $k_{ST} \approx 2$ $k_{IC} \approx 0.1$	($\lambda_{ex} = 436$ nm) $k_{ST} = 2.8$	
425	$k^+ = 2.27$ $k_{ST} \approx 2.1$ $k_{IC} \approx 0.2$		
400	$k^+ = 2.94$ $k_{ST} = 2.4$ $k_{IC} = 0.5$	($\lambda_{ex} = 405$ nm) $k_{ST} = 6.1$	
385	$k^+ = 3.35$ $k_{ST} \approx 2.6$ $k_{IC} \approx 0.8$		
366	$k^+ = 4.13$ $k_{ST} \approx 2.8$ $k_{IC} \approx 1.3$	$k^+ = 8.4$ $k_{ST} = 6.5$ $k_D = 1.9$	$k_D = 2$
337	$k^+ = 7.76$ $k_D \approx 4.5$	$k^+ = 22$	$k^+ \approx 15.4$ $k_{ST} = 10$ $k_D = 54$ ($\lambda_{ex} = 334$ nm)

5. Conclusion

The present results complement McIntosh's work on the HFB fluorescence quantum yield measurements. The lifetime measurements of the S_1 excited state in collision-free conditions clearly show the importance of the internal conversion process at high excitation energies ($\lambda_{ex} \geqslant 400$ nm). We have been able to observe the fluorescence decay in collision-free conditions up to an excitation energy of 30000 cm^{-1}. These results confirm those obtained by Van der Werf and Kommandeur [6] on biacetyl.

Moreover, we notice that, although the total non-radiative rate constant differs by a factor of 4 between biacetyl and HFB, its dependence on excitation energy over the same spectral range (22000 - 27300 cm^{-1}) is essentially the same (a factor of 2 in both cases). In order to determine the fluorescence lifetime of well-defined vibronic levels of the S_1 state we are at present studying the HFB molecule in a supersonic nozzle beam. Under such conditions, after the pulse excitation of a well-defined state of a vibrationally and rotationally cooled collision-free molecule, the time evolution of long-lived

excited species may be studied and a slow fluorescence component may be observed.

Acknowledgments

References

1 S. H. Lin (ed.), *Radiationless Transitions*, Academic Press, New York, 1980, p. 48.
2 C. S. Parmenter and H. M. Poland, *J. Chem. Phys., 51* (1969) 1551.
3 H. W. Sidebottom, C. C. Badcock, J. G. Calvert, B. R. Rabe and E. K. Damon, *J. Am. Chem. Soc., 94* (1972) 13.
   C. C. Badcock, H. W. Sidebottom, J. G. Calvert, B. R. Rabe and E. K. Damon, *J. Am. Chem. Soc., 94* (1972) 19.
4 G. M. McClelland and J. T. Yardley, *J. Chem. Phys., 58* (1973) 4368.
5 M. Bixon and J. Jortner, *J. Chem. Phys., 48* (1968) 715.
6 R. Van der Werf and J. Kommandeur, *Chem. Phys., 16* (1976) 125.
7 F. Lahmani, A. Tramer and C. Tric, *J. Chem. Phys., 60* (1974) 4431.
8 R. Van der Werf, E. Schutten and J. Kommandeur, *Chem. Phys., 11* (1975) 2811.
9 J. S. E. McIntosh and G. B. Porter, *J. Chem. Phys., 48* (12) (1968) 5475.
   J. S. E. McIntosh and G. B. Porter, *Trans. Faraday Soc., 64* (1968) 119.
   J. S. E. McIntosh, *Ph.D. Thesis*, University of British Columbia, 1965.
10 G. B. Porter and W. J. Reid, *J. Photochem., 3* (1974) 27.
   W. J. Reid, *Ph.D. Thesis*, University of British Columbia, 1972.
11 A. L. Henne and P. Trott, *J. Am. Chem. Soc., 69* (1947) 1820.
12 C. O. Moore and J. W. Clark, *U.S. Patent 305, 591, 3,* 1962.
13 A. Petit, F. Launay and J. Rostas, *Appl. Opt., 17* (1978) 3081.
14 A. V. Pocius and J. T. Yardley, *J. Chem. Phys., 61* (9) (1974) 3587.
15 P. A. Hackett and K. O. Kutschke, *J. Phys. Chem., 81* (1977) 1245.
16 A. M. Halpern and W. R. Ware, *J. Chem. Phys., 53* (1970) 1969.
17 W. R. Ware and M. L. Dutton, *J. Chem. Phys., 47* (11) (1967) 4670.
18 W. R. Ware and B. A. Baldwin, *J. Chem. Phys., 40* (6) (1964) 1703.
19 J. B. Birks and D. J. Dyson, *Proc. R. Soc. London, Ser. A, 275* (1963) 135.
20 J. B. Birks, *Photophysics of Aromatic Molecules*, Wiley, New York, 1970.
21 R. A. Marcus, *J. Chem. Phys., 20* (1952) 352.
22 P. C. Haarhoff, *Mol. Phys., 7* (1963) 101.
23 J. W. Sidman and D. S. McClure, *J. Am. Chem. Soc., 77* (1955) 6461, 6471.
24 P. G. Bowers, *Can. J. Chem., 46* (1968) 307.
25 G. R. Fleming, O. L. J. Gijzeman and S. H. Lin, *Chem. Phys. Lett., 21* (3) (1973) 527.

Appendix A

Calculation of the vibrational level densities

We have recorded IR and Raman spectra and the results will be published elsewhere [A1]. The analysis has been made by comparison with related

species (acetone, hexafluoroacetone [A2], glyoxal, oxalyl fluoride, biacetyl [A3 - A5] and trifluoroacetyl chloride [A6]).

The frequencies for the ground state are as follows (in wavenumbers).

CF_3 stretching: 1344; 1272; 1252; 1220; 1200; 1117.

CF_3 deformation: 730; 710; 532; 518; 460; 448.

CF_3 rocking: 305; 293; 245; 180.

C=O stretching: 1779; 1770.

In-plane skeletal stretching: 760; 865 (F_3C—CO); 743 (C—C central bond stretching).

In-plane skeletal bending, C=O wagging: 427; 295; 221; 200. (The last frequency has been evaluated by comparison with oxalyl fluoride [A4, A5].)

Out-of-plane skeletal deformation (C—C—C): 385; 290.

C—C central bond torsion: 100 (given by analogy with biacetyl oxalyl fluoride and biacetyl [A4]).

CF_3 torsion: 70; 70 (taken to be the same as those for hexafluoroacetone [A2]).

References for Appendix A

A1 D. Doisi and A. Petit, to be published (Commissariat à l'Energie Atomique).
A2 C. V. Berney, *Spectrochim. Acta, 21* (1965) 1809.
A3 K. Noack and R. N. Jones, *Can. J. Chem., 39* (1961) 2225.
    W. G. Pateley, R. K. Harris, F. A. Miller and R. E. Witkowski, *Spectrochim. Acta, 21* (1965) 231.
    W. G. Fateley and F. A. Miller, *Spectrochim. Acta, 18* (1962) 977.
A4 J. R. Durig, S. C. Brown and S. E. Hannum, *J. Chem. Phys., 54* (10) (1971) 4428.
A5 J. L. Hencher and G. W. King, *J. Mol. Spectrosc., 16* (1965) 168.
A6 C. V. Berney, *Spectrochim. Acta, 20* (1964) 1437.